# Stochastically Optimal Epipole Estimation in Omnidirectional Images with Geometric Algebra

Christian Gebken and Gerald Sommer

Institute of Computer Science
Chair of Cognitive Systems
Christian-Albrechts-University of Kiel, Germany

{chg,gs}@ks.informatik.uni-kiel.de

**Abstract.** We consider the epipolar geometry between two omnidirectional images acquired from a single viewpoint catadioptric vision sensor with parabolic mirror. This work in particular deals with the estimation of the respective epipoles. We use conformal geometric algebra to show the existence of a $3\times3$ essential matrix, which describes the underlying epipolar geometry. The essential matrix is preferable to the $4\times4$ fundamental matrix, which comprises the fixed intrinsic parameters, as it can be estimated from less data. We use the essential matrix to obtain a prior for a stochastic epipole computation being a key aspect of our work. The computation uses the well-tried amalgamation of a least-squares adjustment (LSA) technique, called the Gauss-Helmert method, with conformal geometric algebra. The imaging geometry enables us to assign distinct uncertainties to the image points which justifies the considerable advantage of our LSA method over standard estimation methods. Next to the stochastically optimal position of the epipoles, the method computes the rigid body motion between the two camera positions. In addition, our text demonstrates the effortlessness and elegance with which such problems integrate into the framework of geometric algebra.

## 1 Introduction

Epipolar geometry is one way to model stereo vision systems. In general, epipolar geometry considers the projection of projection rays from different cameras. The resulting image curve is called epipolar line. The projection of a focal point of another camera is called epipole. Certainly, all epipolar lines must pass through the epipoles. The advantage of epipolar geometry is the search space reduction when doing stereo correspondence analysis: given a pixel in one image the corresponding pixel (if not occluded) must be located on the respective epipolar line. This relation is also expressed by the singular fundamental matrix $\mathsf{F}$, the quadratic form of which attains zero in case a left-image pixel lies on the epipolar line belonging to the right-image pixel, and vice versa. The fundamental matrix contains all geometric information necessary, that is intrinsic and extrinsic parameters, for establishing correspondences between two images. If the intrinsic parameters as focal length, CCD-chip size or the coordinates of the optical center are known, the so-called essential matrix $\mathsf{E}$ describes the imaging in terms

of normalized image coordinates, cf. [10]. The aim of this work is to recover the epipoles, which includes the epipolar geometry, in case of an omnidirectional stereo vision system.

Single viewpoint catadioptric vision sensors combine a conventional camera with one or two mirrors and provide a panoramic view of 360°. Our device is a folded system consisting of two parabolic mirrors and a lens to provide a scaled, approximately orthographic projection from the main mirror, see section 4. According to the work of Nayar et al [8] we can equivalently treat our vision sensor as a single mirror device.

Our initial motivation was to compute a dense 3D-reconstruction from two omnidirectional images. This requires an exact knowledge of the underlying epipolar geometry. We decided on the least-squares adjustment technique called Gauss-Helmert method to account for the invariable uncertainties in observational data. In this way the drawback of nonuniform sampling of the vision sensor turns into an advantage as we can assign distinct uncertainties to the image points depending on their position. Specifically, we do motion estimation from which we ultimately infer the positions of the epipoles. They may then be used for a stereo matching with subsequent 3D-reconstruction. Due to the linearity in the stochastic estimation we have to provide a rough initial estimate for the motion which we refer to as rigid body motion (RBM): in section 5 we derive a formula for the essential matrix $\mathsf{E}$ for the omnidirectional case. In the following we do not explicitly evaluate $\mathsf{E}$ but estimate it from a set of pairs of corresponding image pixels[1]. As the essential matrix reflects the epipolar geometry, we can construct the required first approximation of the RBM from $\mathsf{E}$.

It is vital to notice that we use conformal geometric algebra (CGA) in every part of this text. The omnidirectional imaging can be ideally described in terms of an inversion being a fundamental operation in CGA. At the same time it provides a favorable framework for the mentioned computation of the uncertainties. Our derivation of $\mathsf{E}$ is founded on geometric concepts deduced in and expressed with CGA, which is a new result. Eventually, the underlying tensor notation of CGA enables the (well-tried) amalgamation of the Gauss-Helmert method and geometry, cf. [11]. Before we explain our proposed method in detail, we give an overview of conformal geometric algebra.

## 2 Geometry with Geometric Algebra

Recently it has been shown [12, 13] that the conformal geometry [9] is very attractive for robot vision. Conformal geometric algebra delivers a representation of the Euclidean space with remarkable features: first, the basic geometric entities of conformal geometry are spheres of dimension $n$. Other geometric entities as points, planes, lines, circles, ... may be constructed easily. These entities are no longer set concepts of a vector space but elements of CGA. Second, the special

[1] We initially perform a feature point based stereo matching yielding 50 correspondences on average.

Euclidean group is a subgroup of the conformal group, which is in CGA an orthogonal group. Therefore, its action on the above mentioned geometric entities is linear. Third, the inversion operation is another subgroup of the conformal group which can be advantageously used in robot vision. Fourth, CGA generalizes the incidence algebra of projective geometry with respect to the above mentioned geometric entities.

For a detailed introduction to geometric algebra (GA) see e.g. [5, 2]. Here we only convey a minimal framework. We consider the geometric algebra $\mathbb{G}_{4,1} = \mathcal{C}\ell(\mathbb{R}^{4,1}) \supset \mathbb{R}^{4,1}$ of the 5D conformal space, cf. [1, 7]. Let $\{\mathbf{e}_1, \mathbf{e}_2, \mathbf{e}_3, \mathbf{e}_+, \mathbf{e}_-\}$ denote the basis of the underlying Minkowski space $\mathbb{R}^{4,1}$, where $\mathbf{e}_1^2 = \mathbf{e}_2^2 = \mathbf{e}_3^2 = \mathbf{e}_+^2 = 1 = -\mathbf{e}_-^2$. We use the common abbreviations $\mathbf{e}_\infty = \mathbf{e}_- + \mathbf{e}_+$ and $\mathbf{e}_o = \frac{1}{2}(\mathbf{e}_- - \mathbf{e}_+)$ for the point at infinity and the origin, respectively. The algebra elements are termed multivectors, which we symbolize by capital bold letters, e.g. $\boldsymbol{A}$. A juxtaposition of algebra elements, like $\boldsymbol{CR}$, indicates their geometric product, being the associative, distributive and noncommutative algebra product. We denote '$\cdot$' and '$\wedge$' the inner and outer (exterior) product, respectively. A point $\boldsymbol{x} \in \mathbb{R}^3 \subset \mathbb{G}_{4,1}$ of the Euclidian 3D-space is mapped to a conformal point (null vector) $\boldsymbol{X}$, with $\boldsymbol{X}^2 = 0$, by the embedding operator $\mathcal{K}$

$$\mathcal{K}(\boldsymbol{x}) \;=\; \boldsymbol{X} \;=\; \boldsymbol{x} + \tfrac{1}{2}\,\boldsymbol{x}^2\mathbf{e}_\infty + \mathbf{e}_o\,. \tag{1}$$

A geometric object, say $\boldsymbol{O}$, can now be defined in terms of its inner product null space $\mathbb{I}(\boldsymbol{O}) = \{\boldsymbol{X} \in \mathbb{R}^{4,1} | \boldsymbol{X} \cdot \boldsymbol{O} = 0\}$. This implies an invariance to scalar multiples $\mathbb{I}(\boldsymbol{O}) = \mathbb{I}(\lambda\boldsymbol{O})$, $\lambda \in \mathbb{R}\backslash\{0\}$. Bear in mind that the object definitions given here remain variable in this respect. Verify that $\boldsymbol{S} = \boldsymbol{s} + \frac{1}{2}(\boldsymbol{s}^2 - r^2)\mathbf{e}_\infty + \mathbf{e}_o$ favorably represents a 2-sphere centered at $\boldsymbol{s} \in \mathbb{R}^3$ with radius $r$. Similarly, if $\boldsymbol{n} \in \mathbb{R}^3$, with $\boldsymbol{n}^2 = 1$, then $\boldsymbol{P} = \boldsymbol{n} + d\,\mathbf{e}_\infty$ represents a plane at a distance $d$ from the origin with orientation $\boldsymbol{n}$. Using these vector valued geometric primitives higher order entities can be built: given two objects, e.g. the planes $\boldsymbol{P}_1$ and $\boldsymbol{P}_2$, their line of intersection $\boldsymbol{L}$ is simply the outer product $\boldsymbol{L} = \boldsymbol{P}_1 \wedge \boldsymbol{P}_2$. The outer product of linearly independent points leads to an alternative representation of CGA entities which is literally dual to the inner product null space representation. The term $\boldsymbol{K} = \boldsymbol{A}_1 \wedge \boldsymbol{A}_2 \wedge \boldsymbol{A}_3 \wedge \boldsymbol{A}_4$, for example, represents the sphere that passes through the points $\{\boldsymbol{A}_1, \boldsymbol{A}_2, \boldsymbol{A}_3, \boldsymbol{A}_4\}$ in that a point $\boldsymbol{X} \in \mathbb{R}^{4,1}$ lies on the sphere *iff* $\boldsymbol{X} \wedge \boldsymbol{K} = 0$. Now let $\boldsymbol{S}$ be the element dual[2] to $\boldsymbol{K}$. It may then be shown that $\boldsymbol{X} \wedge \boldsymbol{K} = 0$ *iff* $\boldsymbol{X} \cdot \boldsymbol{S} = 0$ and hence $\boldsymbol{X} \in \mathbb{I}(\boldsymbol{S})$; especially $\{\boldsymbol{A}_1, \boldsymbol{A}_2, \boldsymbol{A}_3, \boldsymbol{A}_4\} \subset \mathbb{I}(\boldsymbol{S})$. Depending on the points the outer product may also yield circles, planes, lines, ...

An important GA operation is the reflection. The reflection of $\boldsymbol{A}$ in a vector valued object $\boldsymbol{O}$ is given by the sandwiching product $\boldsymbol{B} = \boldsymbol{OAO}$. The most general case is the reflection in a sphere, which actually represents an inversion. Note that any RBM can be represented by consecutive reflections in planes. In CGA the resulting elements, for example $\boldsymbol{M} = \boldsymbol{P}_1\boldsymbol{P}_2$, are generally referred to as

[2] Although the role of the dual operation is paramount in GA, cf. [2, 5], it is only touched on in this text. Building the dual of a multivector amounts to a multiplication with the pseudoscalar $\boldsymbol{I} = \mathbf{e}_1\mathbf{e}_2\mathbf{e}_3\mathbf{e}_+\mathbf{e}_-$, $\boldsymbol{I}^2 = -1$.

motors, cf. [12]. Some object $\boldsymbol{C}$ would then be subjected to $\boldsymbol{M}\boldsymbol{C}\widetilde{\boldsymbol{M}}$, whereby the symbol '$\widetilde{\ }$' stands for an order reversion, i.e. the reverse of $\boldsymbol{M}$ is $\widetilde{\boldsymbol{M}} = \boldsymbol{P}_2\boldsymbol{P}_1$. In case of only two involved planes we distinguish between a translator $\boldsymbol{T}$ (parallel planes) and a rotor $\boldsymbol{R}$ (intersecting planes). Note that every motor satisfies the unitarity condition $\boldsymbol{M}\widetilde{\boldsymbol{M}} = \mathbf{1}$. Since reflection is an involution, a double reflection $\boldsymbol{O}(\boldsymbol{O}\boldsymbol{A}\boldsymbol{O})\boldsymbol{O}$ must be the identity w.r.t $\mathbb{I}(\boldsymbol{A})$, therefore $\boldsymbol{O}^2 \in \mathbb{R}$ by associativity. It looks like a conclusion, but in GA every vector valued element $\boldsymbol{X} \in \mathbb{R}^{4,1}$ squares to a scalar by definition $\boldsymbol{X}^2 := \boldsymbol{X} \cdot \boldsymbol{X} \in \mathbb{R}$. Using the above definitions, we have $\boldsymbol{S}^2 = r^2$ and $\boldsymbol{P}^2 = 1$.

### 2.1 Geometric Algebra and its Tensor Notation

We take a look beyond the symbolic level and question how we can realize the structure of geometric algebra numerically. We show a way that makes direct use of the tensor representation inherent in GA.

If $\{\boldsymbol{E}_1, \boldsymbol{E}_2, \ldots, \boldsymbol{E}_{2^n}\}$ denotes the $2^n$-dimensional algebra basis of $\mathbb{G}_n$, then a multivector $\boldsymbol{A} \in \mathbb{G}_n$ can be written as $\boldsymbol{A} = \mathsf{a}^i\,\boldsymbol{E}_i$, where $\mathsf{a}^i$ denotes the $i^{th}$ component of a vector[3] $\mathsf{a} \in \mathbb{R}^{2^n}$ and a sum over the repeated index $i$ is implied. We use this Einstein summation convention also in the following. If $\boldsymbol{B} = \mathsf{b}^i\,\boldsymbol{E}_i$ and $\boldsymbol{C} = \mathsf{c}^i\,\boldsymbol{E}_i$, then the components of $\boldsymbol{C}$ in the algebra equation $\boldsymbol{C} = \boldsymbol{A} \circ \boldsymbol{B}$ can be evaluated via $\mathsf{c}^k = \mathsf{a}^i\,\mathsf{b}^j\,\mathsf{G}^k_{ij}$. Here $\circ$ is a placeholder for the algebra product and $\mathsf{G}^k_{ij} \in \mathbb{R}^{2^n \times 2^n \times 2^n}$ is a tensor encoding this product (we use sans serif letters as $\mathsf{a}, \mathsf{g}$ or $\mathsf{G}$ to denote vectors, matrices, tensors or generally any regular arrangement of numbers). If we define the matrices $\mathsf{U}, \mathsf{V} \in \mathbb{R}^{2^n \times 2^n}$ as $\mathsf{U}(\mathsf{a}) := \mathsf{a}^i\,\mathsf{G}^k_{ij}$ and $\mathsf{V}(\mathsf{b}) := \mathsf{b}^j\,\mathsf{G}^k_{ij}$, then $\mathsf{c} = \mathsf{U}(\mathsf{a})\,\mathsf{b} = \mathsf{V}(\mathsf{b})\,\mathsf{a}$. This perfectly reveals the bilinearity of algebra products.

We define a mapping $\Phi$ and can then write $\Phi(\boldsymbol{A}) = \mathsf{a}$, $\Phi(\boldsymbol{A}\circ) = \mathsf{U}$, $\Phi(\boldsymbol{A}\circ\boldsymbol{B}) = \mathsf{a}^i\,\mathsf{b}^j\,\mathsf{G}^k_{ij}$ or if $\boldsymbol{a} = \mathsf{a}^i\mathbf{e}_i$ is an element of a Euclidian vector space, $\Phi(\boldsymbol{a}) = \mathsf{a}$ as well. Note that we reduce the complexity of equations considerably by only mapping those components of multivectors that are actually needed. As an example, a vector in $\mathbb{G}_n$ can have at most $n$ non-zero components. Also, the outer product of two vectors will not produce 3-vector components, which can thus be disregarded. In the following we assume that $\Phi$ maps to the minimum number of components necessary.

### 2.2 Conformal Embedding - the Stochastic Supplement

We have to obey the rules of error propagation when we embed points by means of function $\mathcal{K}$, equation (1). Assume that point $\boldsymbol{x}$ is a random vector with a Gaussian distribution and $\bar{\boldsymbol{x}}$ is its mean value. Furthermore, we denote the $3\times3$ covariance matrix of $\boldsymbol{x}$ by $\Sigma_{\boldsymbol{x}}$. Let $\mathcal{E}$ denote the expectation value operator, such that $\mathcal{E}[\boldsymbol{x}] = \bar{\boldsymbol{x}}$. The uncertain representative in conformal space, i.e. the

[3] At least numerically, there is no other way than representing multivectors as vectors.

stochastic supplement for $\boldsymbol{X} = \mathcal{K}(\bar{\boldsymbol{x}})$, is determined by a sphere with imaginary radius

$$\mathcal{E}\big[\mathcal{K}(\boldsymbol{x})\big] \;=\; \bar{\boldsymbol{x}} + \tfrac{1}{2}\,\bar{\boldsymbol{x}}^2\,\mathbf{e}_\infty + \;\mathbf{e}_o \;+\; \tfrac{1}{2}\mathrm{trace}\big(\Sigma_{\boldsymbol{x}}\big)\mathbf{e}_\infty \tag{2}$$

rather than the pure conformal point $\mathcal{K}\big(\mathcal{E}[\boldsymbol{x}]\big)$. However, in accordance with [11] we refrain from using the exact term since the advantages of conformal points over spheres with imaginary radius outbalance the numerical error.

We evaluate the corresponding $5\times5$ covariance matrix $\Sigma_{\boldsymbol{X}}$ for $\boldsymbol{X} = \mathcal{K}(\bar{\boldsymbol{x}})$ by means of error propagation and find

$$\Sigma_{\boldsymbol{X}} = \mathsf{J}_{\mathcal{K}}(\bar{\boldsymbol{x}})\;\Sigma_{\boldsymbol{x}}\;\mathsf{J}_{\mathcal{K}}^{\mathsf{T}}(\bar{\boldsymbol{x}})\,, \tag{3}$$

where we used the Jacobian of $\mathcal{K}$

$$\mathsf{J}_{\mathcal{K}}(\bar{\boldsymbol{x}}) := \frac{\partial\mathcal{K}}{\partial\boldsymbol{X}} = \begin{bmatrix} 1 & 0 & 0 \\ 0 & 1 & 0 \\ 0 & 0 & 1 \\ \bar{x}_1 & \bar{x}_2 & \bar{x}_3 \\ 0 & 0 & 0 \end{bmatrix}. \tag{4}$$

## 3 Stochastic Estimation Method

In the field of parameter estimation one usually parameterizes some physical process $\mathcal{P}$ in terms of a model $\mathcal{M}$ and a suitable parameter vector $\mathsf{p}$. The components of $\mathsf{p}$ are then to be estimated from a set of observations originating from $\mathcal{P}$.

Here, we introduce our two parameter estimation methods, the common Gauss-Markov method and the most generalized case of least squares adjustment, the Gauss-Helmert method. Both are founded on the respective homonymic linear models, cf. [6]. The word 'adjustment' puts emphasis on the fact that an estimation has to handle redundancy in observational data appropriately, i.e. to weight unreliable data to a lesser extent. In order to overcome the inherent noisiness of measurements one typically introduces a redundancy by taking much more measurements than necessary to describe the process. Each observation must have its own covariance matrix describing the corresponding Gaussian probability density function that is assumed to model the observational error. The determination of which is inferred from the knowledge of the underlying measurement process. The matrices serve as weights and thereby introduce a local error metric.

The principle of least squares adjustment, i.e. to minimize the sum of squared weighted errors $\Delta\mathsf{y}_i$, is often denoted as

$$\sum_i \Delta\mathsf{y}_i^{\mathsf{T}}\,{\Sigma_{\mathsf{y}_i}}^{-1}\Delta\mathsf{y}_i \;\longrightarrow\; \min\,, \tag{5}$$

where $\Sigma_{\mathsf{y}_i}$ is a covariance matrix assessing the confidence of $\mathsf{y}_i$.

Let $\{\mathsf{b}_1, \mathsf{b}_2, \ldots, \mathsf{b}_N\}$ be a set of $N$ observations, for which we introduce the abbreviation $\{\mathsf{b}_{1\ldots N}\}$. Each observation $\mathsf{b}_i$ is associated with an appropriate covariance matrix $\Sigma_{\mathsf{b}_i}$. An entity, parameterized by a vector $\mathsf{p}$, is to be fitted to the

observational data. Consequently, we define a condition function $\mathsf{g}(\mathsf{b}_i,\, \mathsf{p})$ which is supposed to be zero if the observations and the entity in demand fit algebraically. Besides, it is often inevitable to define constraints $\mathsf{h}(\mathsf{p}) = \mathsf{0}$ on the parameter vector $\mathsf{p}$. This is necessary if there are functional dependencies within the parameters. Consider, for example, the parameterization of a Euclidean normal vector $\mathsf{n}$ using three variables $\mathsf{n} = [n_1, n_2, n_3]^\mathsf{T}$. A constraint $\mathsf{n}^\mathsf{T}\mathsf{n} = 1$ could be avoided using spherical coordinates $\theta$ and $\phi$, i.e. $\mathsf{n} = [\cos\theta\cos\phi, \cos\theta\sin\phi, \sin\theta]^\mathsf{T}$. In the following sections, we refer to the functions $\mathsf{g}$ and $\mathsf{h}$ as G-constraint and H-constraint, respectively.

Note that most of the fitting problems in these sections are not linear but quadratic, i.e. the condition equations require a linearization and estimation becomes an iterative process. An important issue is thus the search for an initial estimate (starting point). If we know an already good estimate $\hat{\mathsf{p}}$, we can make a linearization of the G-constraint yielding $(\partial_\mathsf{p}\,\mathsf{g})(\mathsf{b}_i,\hat{\mathsf{p}})\Delta\mathsf{p} + \mathsf{g}(\mathsf{b}_i,\, \hat{\mathsf{p}}) \approx \mathsf{0}$. Hence, with $\mathsf{U}_i = (\partial_\mathsf{p}\,\mathsf{g})(\mathsf{b}_i,\hat{\mathsf{p}})$ and $\mathsf{y}_i = -\mathsf{g}(\mathsf{b}_i,\, \hat{\mathsf{p}})$: $\mathsf{U}_i\Delta\mathsf{p} = \mathsf{y}_i + \Delta\mathsf{y}_i$, which exactly matches the linear Gauss-Markov model. The minimization of equation (5) in conjunction with the Gauss-Markov model leads to the best linear unbiased estimator. Note that we have to leave the weighting out in equation (5), since our covariance matrices $\Sigma_{\mathsf{b}_i}$ do not match the $\Sigma_{\mathsf{y}_i}$. Subsequently, we consider a model which includes the weighting.

If we take our observations as estimates, i.e. $\{\hat{\mathsf{b}}_{1\ldots N}\} = \{\mathsf{b}_{1\ldots N}\}$, we can make a Taylor series expansion of first order at $(\hat{\mathsf{b}}_i,\, \hat{\mathsf{p}})$ yielding

$$(\partial_\mathsf{p}\,\mathsf{g})(\hat{\mathsf{b}}_i,\hat{\mathsf{p}})\Delta\mathsf{p} + (\partial_\mathsf{b}\,\mathsf{g})(\hat{\mathsf{b}}_i,\hat{\mathsf{p}})\Delta\mathsf{b}_i + \mathsf{g}(\hat{\mathsf{b}}_i,\, \hat{\mathsf{p}}) \approx \mathsf{0}\,. \tag{6}$$

Similarly, with $\mathsf{V}_i = (\partial_\mathsf{b}\,\mathsf{g})(\hat{\mathsf{b}}_i,\hat{\mathsf{p}})$ we obtain $\mathsf{U}_i\Delta\mathsf{p} + \mathsf{V}_i\Delta\mathsf{b}_i = \mathsf{y}_i$, which exactly matches the linear Gauss-Helmert model. Note that the error term $\Delta\mathsf{y}_i$ has been replaced by the linear combination $\Delta\mathsf{y}_i = -\mathsf{V}_i\Delta\mathsf{b}_i$; the Gauss-Helmert differs from the Gauss-Markov model in that the observations have become random variables and are thus allowed to undergo small changes $\Delta\mathsf{b}_i$ to compensate for errors. But changes have to be kept minimal, as observations represent the best available. This is achieved by replacing equation (5) with

$$\sum_i \Delta\mathsf{b}_i^\mathsf{T}\,{\Sigma_{\mathsf{b}_i}}^{-1}\Delta\mathsf{b}_i \;\longrightarrow\; \min\,, \tag{7}$$

where $\Delta\mathsf{b}_i$ is now considered as error vector.

The minimization of (7) subject to the Gauss-Helmert model can be done using Lagrange multipliers. By introducing $\Delta\mathsf{b} = [\Delta\mathsf{b}_1^\mathsf{T}, \Delta\mathsf{b}_2^\mathsf{T}, \ldots, \Delta\mathsf{b}_N^\mathsf{T}]^\mathsf{T}$, $\Sigma_\mathsf{b} = \mathtt{diag}([\Sigma_{\mathsf{b}_1}, \Sigma_{\mathsf{b}_2}, \ldots, \Sigma_{\mathsf{b}_N}])$, $\mathsf{U} = [\mathsf{U}_1^\mathsf{T}, \mathsf{U}_2^\mathsf{T}, \ldots, \mathsf{U}_N^\mathsf{T}]^\mathsf{T}$, $\mathsf{V} = \mathtt{diag}([\mathsf{V}_1, \mathsf{V}_2, \ldots, \mathsf{V}_N])$ and $\mathsf{y} = [\mathsf{y}_1^\mathsf{T}, \mathsf{y}_2^\mathsf{T}, \ldots, \mathsf{y}_N^\mathsf{T}]^\mathsf{T}$ the Lagrange function $\Psi$, which is now to be minimized, becomes

$$\Psi(\Delta\mathsf{p},\, \Delta\mathsf{b},\, \mathsf{u},\, \mathsf{v}) \;=\; \frac{1}{2}\,\Delta\mathsf{b}^\mathsf{T}\,{\Sigma_\mathsf{b}}^{-1}\,\Delta\mathsf{b} - \Big(\,\mathsf{U}\,\Delta\mathsf{p}+\mathsf{V}\,\Delta\mathsf{b}-\mathsf{y}\,\Big)^\mathsf{T}\mathsf{u} + \Big(\,\mathsf{H}\,\Delta\mathsf{p}-\mathsf{z}\,\Big)^\mathsf{T}\mathsf{v}\,. \tag{8}$$

The last summand in $\Psi$ corresponds to the linearized H-constraint, where $\mathsf{H} = (\partial_\mathsf{p}\mathsf{h})(\hat{\mathsf{p}})$ and $\mathsf{z} = -\,\mathsf{h}(\hat{\mathsf{p}})$ was used. That term can be omitted, if $\mathsf{p}$ has no functional dependencies. A differentiation of $\Psi$ with respect to all variables gives an

extensive matrix equation, which could already be solved. Nevertheless, it can be considerably reduced with the substitutions $\mathsf{N} = \sum_i \mathsf{U}_i^\mathsf{T} \left(\mathsf{V}_i \ \Sigma_{\mathsf{b}_i} \ \mathsf{V}_i^\mathsf{T}\right)^{-1} \mathsf{U}_i$ and $\mathsf{z}_N = \sum_i \mathsf{U}_i^\mathsf{T} \left(\mathsf{V}_i \ \Sigma_{\mathsf{b}_i} \ \mathsf{V}_i^\mathsf{T}\right)^{-1} \mathsf{y}$. The resultant matrix equation is free from $\Delta\mathsf{b}$ and can be solved for $\Delta\mathsf{p}$

$$\begin{bmatrix} \mathsf{N} & \mathsf{H}^\mathsf{T} \\ \mathsf{H} & 0 \end{bmatrix} \begin{bmatrix} \Delta\mathsf{p} \\ \mathsf{v} \end{bmatrix} = \begin{bmatrix} \mathsf{z}_N \\ \mathsf{z} \end{bmatrix} . \tag{9}$$

For the corrections $\{\Delta\mathsf{b}_{1\ldots N}\}$, which are now minimal with respect to the Mahalanobis distance (7), we compute

$$\Delta\mathsf{b}_i = \Sigma_{\mathsf{b}_i}\mathsf{V}_i^\mathsf{T} \left(\mathsf{V}_i\Sigma_{\mathsf{b}_i}\mathsf{V}_i^\mathsf{T}\right)^{-1} \left(\mathsf{y}_i - \mathsf{U}_i\,\Delta\mathsf{p}\right). \tag{10}$$

It is an important by-product that the (pseudo-) inverse of the quadratic matrix in equation (9) contains the covariance matrix $\Sigma_{\Delta\mathsf{p}} = \Sigma_\mathsf{p}$ belonging to $\mathsf{p}$. The similar solution for the Gauss-Markov model and the corresponding proofs and derivations can be found in [6].

## 4 Omnidirectional Imaging

Consider a camera, focused at infinity, which looks upward at a parabolic mirror centered on its optical axis. This setup is shown in figure 1. A light ray emitted

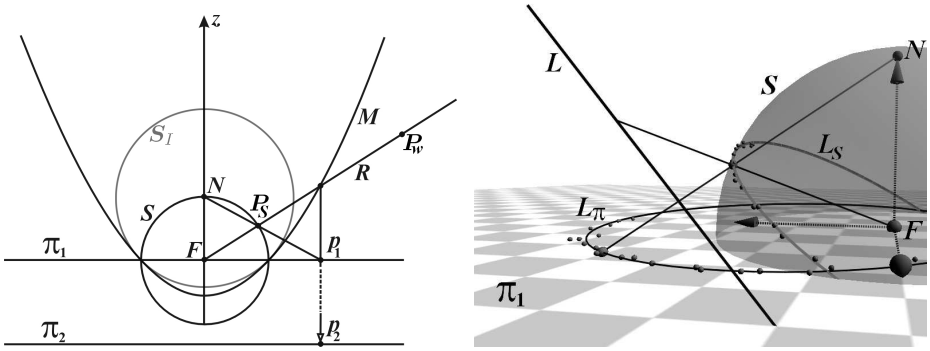


**Fig. 1.** Left: mapping (cross-section) of a world point $\boldsymbol{P}_w$: the image planes $\boldsymbol{\pi}_1$ and $\boldsymbol{\pi}_2$ are identical. Right: mapping of line $\boldsymbol{L}$ to $\boldsymbol{L}_\pi$ via great circle $\boldsymbol{L}_\boldsymbol{S}$ on $\boldsymbol{S}$.

from world point $\boldsymbol{P}_w$ that would pass through the focal point $\boldsymbol{F}$ of the parabolic mirror $M$, is reflected parallel to the central axis of $M$, to give point $\boldsymbol{p}_2$ on image plane $\boldsymbol{\pi}_2$. Now we use the simplification that a projection to sphere $\boldsymbol{S}$ with a subsequent stereographic projection to $\boldsymbol{\pi}_1$ produces a congruent image on $\boldsymbol{\pi}_1$. Accordingly, point $\boldsymbol{P}_w$ maps to $\boldsymbol{P}_S$ and further to $\boldsymbol{p}_1$, see figure 1. Together

with the right side of figure 1 it is intuitively clear that infinitely extended lines form great circles on $\boldsymbol{S}$. Moreover, a subsequent stereographic projection, being a conformal mapping, results in circles on the image plane which then are no more concentric. For details refer to [4].

Note that the stereographic projection can also be done in terms of an inversion in a suitable sphere $\boldsymbol{S}_I$ centered at the North Pole $\boldsymbol{N}$ of $\boldsymbol{S}$. For the scenario depicted in figure 1 one can easily verify that the radius of $\boldsymbol{S}_I$ must be $\sqrt{2}\,r$, if $r$ denotes the radius of $\boldsymbol{S}$. Using CGA we have $\boldsymbol{P}_S = \boldsymbol{S}_I \boldsymbol{p}_1 \boldsymbol{S}_I$.

## 5 Discovering Catadioptric Stereo Vision with CGA

We now formulate a condition for the matching of image points. This enables the derivation of the fundamental matrix $\mathsf{F}$ and the essential matrix $\mathsf{E}$ for the parabolic catadioptric case.

Consider the stereo setup of figure 2 in which the imaging of world point $\boldsymbol{P}_w$ is depicted. Each of the projection spheres $\boldsymbol{S}$ and $\boldsymbol{S}'$ represents the catadioptric imaging device. The interrelating 3D-motion is denoted RBM (rigid body motion). Note that the left coordinate system is also rotated about the vertical axis.

The two projections of $\boldsymbol{P}_w$ are $\boldsymbol{X}$ and $\boldsymbol{Y}'$. Let $\boldsymbol{x}$ and $\boldsymbol{y}$ be their respective image points (on the image plane). The inverse stereographic projection of $\boldsymbol{x}$ and $\boldsymbol{y}$ yields the points $\boldsymbol{X}$ and $\boldsymbol{Y}$, which here share the camera coordinate system centered at $\boldsymbol{F}$. In order to do stereo our considerations must involve the RBM, that we denote by the motor $\boldsymbol{M}$ from now on. Hence we can write $\boldsymbol{Y}' = \boldsymbol{M}\boldsymbol{Y}\widetilde{\boldsymbol{M}}$ and so $\{\boldsymbol{S}', \boldsymbol{F}'\} = \boldsymbol{M}\{\boldsymbol{S}, \boldsymbol{F}\}\widetilde{\boldsymbol{M}}$.

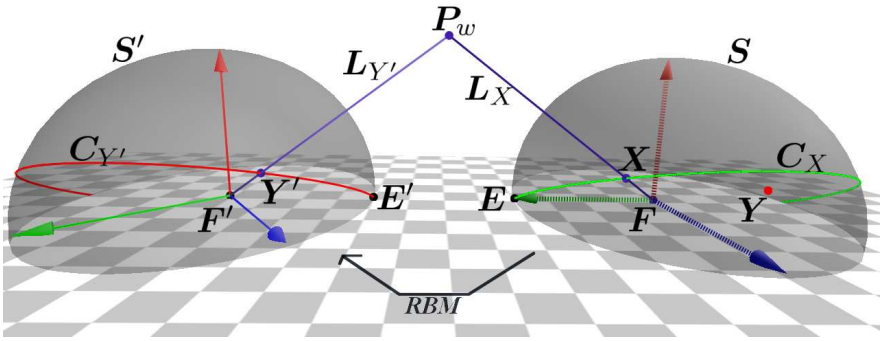


**Fig. 2.** Omnidirectional stereo vision: the projection of ray $\boldsymbol{L}_X$ ($\boldsymbol{L}_{Y'}$) is the great circle $\boldsymbol{C}_{Y'}$ ($\boldsymbol{C}_X$). The 3D-epipole $\boldsymbol{E}$ ($\boldsymbol{E}'$) is the projection of the focal point $\boldsymbol{F}'$ ($\boldsymbol{F}$).

As we already know from section 4, lines project to great circles; the projection of $\boldsymbol{L}_X$ on $\boldsymbol{S}'$, for example, is the circle $\boldsymbol{C}_{Y'}$ including $\boldsymbol{Y}'$. This motivates the

underlying epipolar geometry since all those great circles must pass through the point $\boldsymbol{E}'$ being the projection of $\boldsymbol{F}$. This must be the case because independent of $\boldsymbol{P}_w$ all triangles $\overline{\boldsymbol{F}\boldsymbol{P}_w\boldsymbol{F}'}$ have the line connecting $\boldsymbol{F}$ and $\boldsymbol{F}'$, called baseline, in common. Subsequently we refer to the 3D-points $\boldsymbol{E}$ and $\boldsymbol{E}'$ as 3D-epipoles.

Intelligibly, the two projection rays $\boldsymbol{L}_X$ and $\boldsymbol{L}_{Y'}$ intersect if the four points $\boldsymbol{F}', \boldsymbol{Y}', \boldsymbol{X}$ and $\boldsymbol{F}$ are coplanar. We express this condition in terms of CGA. The outer product of four conformal points, say $\boldsymbol{A}_1, \boldsymbol{A}_2, \boldsymbol{A}_3$ and $\boldsymbol{A}_4$, results in the sphere $\boldsymbol{K}_A = \boldsymbol{A}_1 \wedge \boldsymbol{A}_2 \wedge \boldsymbol{A}_3 \wedge \boldsymbol{A}_4$ comprising the points. If these are coplanar the sphere degenerates to the special sphere with infinite radius - which is a plane. Recall from section 2 that a plane lacks the $\mathbf{e}_o$-component in contrast to a sphere. The explanation is that the $\mathbf{e}_o$-component carries the value $(\boldsymbol{a}_2 - \boldsymbol{a}_1) \wedge (\boldsymbol{a}_3 - \boldsymbol{a}_1) \wedge (\boldsymbol{a}_4 - \boldsymbol{a}_1)$ which amounts to the triple product $(\boldsymbol{a}_2 - \boldsymbol{a}_1) \cdot ((\boldsymbol{a}_3 - \boldsymbol{a}_1) \times (\boldsymbol{a}_4 - \boldsymbol{a}_1))$, where $\boldsymbol{A}_i = \mathcal{K}(\boldsymbol{a}_i \in \mathbb{R}^3)$, $1 \leq i \leq 4$. Our condition must therefore ensure the $\mathbf{e}_o^*$-component[4] to be zero

$$\boldsymbol{G} \;=\; \boldsymbol{F} \wedge \boldsymbol{X} \wedge \boldsymbol{F}' \wedge \boldsymbol{Y}' \;=\; (\boldsymbol{F} \wedge \boldsymbol{X}) \;\wedge\; \boldsymbol{M}\big(\boldsymbol{F} \wedge \boldsymbol{Y}\big)\widetilde{\boldsymbol{M}} \quad \overset{\mathbf{e}_o^*}{=} \quad 0\,. \tag{11}$$

Using the abbreviations $\underline{\boldsymbol{X}} = \boldsymbol{F} \wedge \boldsymbol{X}$ and $\underline{\boldsymbol{Y}} = \boldsymbol{F} \wedge \boldsymbol{Y}$ the upper formula reads $\boldsymbol{G} = \underline{\boldsymbol{X}} \wedge \boldsymbol{M}\underline{\boldsymbol{Y}}\widetilde{\boldsymbol{M}} \overset{\mathbf{e}_o^*}{=} 0$. We now exploit the tensor representation introduced in section 2.1 and obtain

$$\mathsf{g}^t(\mathsf{m}, \underline{\mathsf{x}}, \underline{\mathsf{y}}) \;=\; \underline{\mathsf{x}}^k \; \mathsf{O}^t_{kc} \; (\mathsf{m}^i \; \mathsf{G}^a_{il} \; \underline{\mathsf{y}}^l \; \mathsf{G}^c_{ab} \; \mathsf{R}^b_j \; \mathsf{m}^j)\,, \tag{12}$$

where $\Phi(\boldsymbol{G}) = \mathsf{g}$, $\Phi(\underline{\boldsymbol{X}}) = \underline{\mathsf{x}}$, $\Phi(\underline{\boldsymbol{Y}}) = \underline{\mathsf{y}}$ and $\Phi(\boldsymbol{M}) = \mathsf{m}$. Note that we only have to take a particular $t = t^*$ into account which indexes to the $\mathbf{e}_o^*$-component of the result. After setting $\boldsymbol{F} = \mathbf{e}_o$ it can be shown that $\underline{\mathsf{x}}$ and $\underline{\mathsf{y}}$ in fact denote the Euclidean 3D-coordinates on the projection spheres, i.e. $\underline{\mathsf{x}}, \underline{\mathsf{y}} \in \mathbb{R}^3$. For the motor $\boldsymbol{M}$ we have $\mathsf{m} \in \mathbb{R}^8$ in CGA, which is an overparameterization as an RBM has six degrees of freedom. The product tensors $\mathsf{O}$, $\mathsf{G}$ and $\mathsf{R}$ denote the outer product, the geometric product and the reverse, respectively. If we fix a motor $\mathsf{m}$ we get the bilinear form $\mathsf{g}(\underline{\mathsf{x}}, \underline{\mathsf{y}}) = \underline{\mathsf{x}}^k \, \mathsf{E}_{kl} \, \underline{\mathsf{y}}^l$ with $\mathsf{E}_{kl} = \mathsf{O}^{t^*}_{kc} \, \mathsf{m}^i \, \mathsf{G}^a_{il} \, \mathsf{G}^c_{ab} \, \mathsf{R}^b_j \, \mathsf{m}^j$. The condition is linear in $\underline{\boldsymbol{X}}$ and linear in $\underline{\boldsymbol{Y}}$ as expected by the bilinearity of the geometric product. Its succinct matrix notation is

$$\underline{\mathsf{x}}^\mathsf{T} \mathsf{E} \, \underline{\mathsf{y}} \;=\; 0\,, \tag{13}$$

where $\mathsf{E} \in \mathbb{R}^{3\times3}$ denotes the essential matrix of the epipolar geometry. We do not give a proof but mention that equation (13), which ultimately reflects a triple product, is zero if and only if there is coplanarity between the four points $\boldsymbol{F}', \boldsymbol{Y}', \boldsymbol{X}$ and $\boldsymbol{F}$. Next, if we set $\boldsymbol{Y}' = \boldsymbol{E}'$ or $\boldsymbol{X} = \boldsymbol{E}$ we get $\mathsf{E}\,\underline{\mathsf{y}} = \mathsf{0}$ and $\underline{\mathsf{x}}^\mathsf{T}\mathsf{E} = \mathsf{0}$, respectively. Otherwise, say $\mathsf{E}\,\underline{\mathsf{y}} = \mathsf{n} \in \mathbb{R}^3$, we could choose an $\boldsymbol{X}$ such that the corresponding $\underline{\mathsf{x}}$ is not orthogonal to $\mathsf{n}$ and get $\underline{\mathsf{x}}^\mathsf{T}\mathsf{E}\,\underline{\mathsf{y}} \neq 0$. This would imply that the points $\boldsymbol{F}', \boldsymbol{E}', \boldsymbol{F}$ and the chosen $\boldsymbol{X}$ are not coplanar, which must be a

[4] The component dual to $\mathbf{e}_o$-component (denoted $\mathbf{e}_o^*$) must be zero as the outer product representation is dual to the sphere representation given in section 2.

contradiction since $\boldsymbol{F}', \boldsymbol{E}'$ and $\boldsymbol{F}$ are already collinear. Hence the 3D-epipoles reflect the left and right nullspace of $\mathsf{E}$ and we can infer that the rank of $\mathsf{E}$ can be at most two.

Because $\mathsf{E}$ does solely depend on the motor $\boldsymbol{M}$, comprising the extrinsic parameters, it can not be a fundamental matrix, which must include the intrinsic parameters as well. Fortunately, we can easily extend our previous derivations to obtain the fundamental matrix $\mathsf{F}$. Recall the image points $\boldsymbol{x}$ and $\boldsymbol{y}$. They are related to $\boldsymbol{X}$ and $\boldsymbol{Y}$ in terms of a stereographic projection. As already stated in section 4, a stereographic projection is equal to an inversion in a certain sphere, but inversion is the most fundamental operation in CGA. In accordance with figure 1 we can write

$$\boldsymbol{X} \;=\; \boldsymbol{S}_I \boldsymbol{X}_\pi \boldsymbol{S}_I \,,$$

where $\boldsymbol{X}_\pi = \mathcal{K}(\boldsymbol{x})$ denotes the conformal embedding of point $\boldsymbol{x}$ on the image plane $\pi$. Note that the inversion sphere $\boldsymbol{S}_I$ depends on the focal length of the parabolic mirror and on the CCD-chip size, i.e. a scaling factor. In this way equation (11) becomes $\boldsymbol{G} = \boldsymbol{F} \wedge (\boldsymbol{S}_I \boldsymbol{X}_\pi \boldsymbol{S}_I) \wedge \boldsymbol{F}' \wedge (\boldsymbol{S}_I \boldsymbol{Y}'_\pi \boldsymbol{S}_I) \overset{\mathbf{e}_o^*}{=} 0$. In addition, the principal point offset (the coordinates of the pixel where the optical axis hits the image plane) can be included by introducing a suitable translator $\boldsymbol{T}_C$. We then would have to replace $\boldsymbol{S}_I$ by the compound operator $\boldsymbol{Z} = \boldsymbol{S}_I \boldsymbol{T}_C$. We would finally obtain

$$\boldsymbol{G} \;=\; \boldsymbol{F} \wedge (\boldsymbol{Z} \boldsymbol{X}_\pi \widetilde{\boldsymbol{Z}}) \wedge \boldsymbol{F}' \wedge (\boldsymbol{Z} \boldsymbol{Y}'_\pi \widetilde{\boldsymbol{Z}}) \quad \overset{\mathbf{e}_o^*}{=} \quad 0 \,. \tag{14}$$

However, equation (14) is still linear in the points $\boldsymbol{X}_\pi$ and $\boldsymbol{Y}_\pi$. We refrain from specifying the corresponding tensor representation or the fundamental matrix, respectively. Instead we show a connection to the work of Geyer and Daniilidis [3]. They have derived a catadioptric fundamental matrix of dimension $4 \times 4$ for what they call lifted image points which live in a 4D-Minkowski space (the fourth basis vector squares to $-1$). The lifting raises an image point $\mathsf{p} = [u, v]^\mathsf{T}$ onto a unit sphere centered at the origin such that the lifted point $\tilde{\mathsf{p}} \in \mathbb{R}^{3,1}$ is collinear with $\mathsf{p}$ and the North Pole $N$ of the sphere. Thus the lifting corresponds to a stereographic projection. The lifting of $\mathsf{p}$ is defined as

$$\tilde{\mathsf{p}} \;=\; [2u, 2v, u^2 + v^2 - 1, u^2 + v^2 + 1]^\mathsf{T} \,. \tag{15}$$

Compare the conformal embedding $\boldsymbol{P} = \mathcal{K}(\mathsf{p}) = u\,\mathbf{e}_1 + v\,\mathbf{e}_2 + \frac{1}{2}(u^2+v^2)\,\mathbf{e}_\infty + 1\;\mathbf{e}_o$ in the $\mathbf{e}_\infty$-$\mathbf{e}_o$-coordinate system ($\Phi$ discards the $\mathbf{e}_3$-coordinate being zero)

$$\Phi(\boldsymbol{P}) = [u, v, \tfrac{1}{2}(u^2 + v^2), 1]^\mathsf{T} \,.$$

We can switch back to the $\mathbf{e}_+$-$\mathbf{e}_-$-coordinate system of the conformal space with the linear (basis) transformation $\mathsf{B}$

$$\mathsf{B}\,\Phi(\boldsymbol{P}) \;=\; \begin{bmatrix} 1 & 0 & 0 & 0 \\ 0 & 1 & 0 & 0 \\ 0 & 0 & 1 & -\frac{1}{2} \\ 0 & 0 & 1 & +\frac{1}{2} \end{bmatrix} \begin{bmatrix} u \\ v \\ \frac{1}{2}(u^2 + v^2) \\ 1 \end{bmatrix} \;=\; \begin{bmatrix} u \\ v \\ \frac{1}{2}(u^2 + v^2 - 1) \\ \frac{1}{2}(u^2 + v^2 + 1) \end{bmatrix} .$$

The lifting in equation (15) is therefore identical to the conformal embedding up to a scalar factor 2. At first, this implies that $\tilde{\boldsymbol{x}} = 2\mathsf{B}\,\Phi(\boldsymbol{X}_\pi) = 2\mathsf{B}\,\Phi(\mathcal{K}(\boldsymbol{x}))$. Second, if $\tilde{\mathsf{F}} \in \mathbb{R}^{4\times4}$ denotes a fundamental matrix for lifted points then, by analogy, $\mathsf{F} = 4\,\mathsf{B}^\mathsf{T}\tilde{\mathsf{F}}\mathsf{B}$ is the fundamental matrix that we would obtain from equation (14).

## 6 Estimating Epipoles

The results of the previous section are now to be applied to the epipole estimation. We use the essential matrix $\mathsf{E}$ to estimate the epipoles for two reasons. First, the intrinsic parameters do not change while the imaging device moves; one initial calibration is enough. Second, the rank-2 essential matrix is only of dimension $3 \times 3$ and one needs at least eight points for the estimation.

We choose nine pairs of corresponding image points. For each image point $\boldsymbol{x}$ we compute $\underline{\mathsf{x}} = \Phi(\,\mathbf{e}_o \wedge \mathcal{K}(\boldsymbol{x})) \in \mathbb{R}^3$. We finally have $\mathbb{X} = \{\underline{\mathsf{x}}_{1\ldots9}\}$ and $\mathbb{Y} = \{\underline{\mathsf{y}}_{1\ldots9}\}$. Every $\underline{\mathsf{x}}$-$\underline{\mathsf{y}}$-pair must satisfy equation (13) which can be rephrased as $\mathtt{vec}(\underline{\mathsf{x}}\underline{\mathsf{y}}^\mathsf{T})^\mathsf{T}\mathtt{vec}(\mathsf{E}) = 0$, where $\mathtt{vec}(\cdot)$ reshapes a matrix into a column vector. Hence the best least-squares approximation of $\mathtt{vec}(\mathsf{E})$ is the right-singular vector to the smallest singular value of the matrix consisting of the row vectors $\mathtt{vec}(\underline{\mathsf{x}}_i\underline{\mathsf{y}}_i^\mathsf{T})^\mathsf{T}$, $1 \le i \le 9$. Let $\check{\mathsf{E}}$ be the estimated essential matrix. The left- and right-singular vectors to the smallest singular value of $\check{\mathsf{E}}$ are then our approximations to the 3D-epipoles, as described above. The epipoles then serve as a prior for the stochastic epipole estimation explained in the following section.

## 7 Stochastic Epipole Estimation

Here we describe the second key contribution of our work. The epipoles computed via the essential matrix are now to be refined. We do so by estimating the interrelating motor $\boldsymbol{M}$, parameterized by $\mathsf{m} \in \mathbb{R}^8$. The direction to the 3D-epipoles can then be extracted from the points $\boldsymbol{M}\boldsymbol{F}\widetilde{\boldsymbol{M}}$ and $\widetilde{\boldsymbol{M}}\boldsymbol{F}\boldsymbol{M}$. Note that the former point equals $\boldsymbol{F}'$. In order to apply the Gauss-Helmert method introduced in section 3 we have to provide the G-constraint, the H-constraint, the observations with associated uncertainties and a rough initial estimate.

As input data we use all $N$ pairs of corresponding points, i.e. we use $\mathbb{X} = \{\underline{\mathsf{x}}_{1\ldots N}\}$ and $\mathbb{Y} = \{\underline{\mathsf{y}}_{1\ldots N}\}$. An observation is a pair $(\underline{\mathsf{x}}_i, \underline{\mathsf{y}}_i)$, $1 \le i \le N$. In our case the G-constraint is simply equation (12) with $t = t^*$

$$g^t(\mathsf{m}, \underline{\mathsf{x}}, \underline{\mathsf{y}}) \;=\; \underline{\mathsf{x}}_n^k\;\mathsf{O}_{kc}^t\;(\mathsf{m}^i\;\mathsf{G}_{il}^a\;\underline{\mathsf{y}}_n^l\;\mathsf{G}_{ab}^c\;\mathsf{R}_j^b\;\mathsf{m}^j), \qquad 1 \le n \le N\,, \tag{16}$$

Hence differentiating with respect to $\underline{\mathsf{x}}$, $\underline{\mathsf{y}}$ and $\mathsf{m}$ yields the required matrices $\mathsf{V}$ and $\mathsf{U}$, respectively. Since an RBM is defined by six rather than eight parameters, we need the H-constraint. To ensure that $\mathsf{m}$ encodes a motor it is sufficient to constrain the unitarity of $\boldsymbol{M}$ by demanding that $\boldsymbol{M}\widetilde{\boldsymbol{M}} = \mathbf{1}$. We also have to constrain that $\boldsymbol{M}$ does not converge to the identity element $\boldsymbol{M} = \mathbf{1}$. Otherwise the condition equation (11) would become $\boldsymbol{G} = \boldsymbol{F} \wedge \boldsymbol{X} \wedge \boldsymbol{F} \wedge \boldsymbol{Y}$ being zero at

all times. This is achieved by constraining the $\mathbf{e}_\infty$-component of $\boldsymbol{F}' = \boldsymbol{M}\boldsymbol{F}\widetilde{\boldsymbol{M}}$, $\boldsymbol{F} = \mathbf{e}_o$, to be 0.5. Thus the distance between $\boldsymbol{F}$ and $\boldsymbol{F}'$ is set to one[5]. The initial estimate $\hat{\mathsf{m}}$ is the unit length translator $\boldsymbol{T}_E$ along the direction of the 3D-epipole $\boldsymbol{E}$, i.e. $\hat{\mathsf{m}} = \Phi(\boldsymbol{T}_E)$.

We assume that all image points initially have the same 2D-uncertainty given by a $2\times2$ identity covariance matrix, i.e. we assume an pixel error of one in row and column. The conformal embedding then adjusts the covariance matrices as explained in section 2.2. Recall that the computation of our observations, say $\underline{\mathsf{x}}$, involves a stereographic projection that we perform by means of an inversion. The points thereby obtain distinct 3D-uncertainties accounting for the imaging geometry. The mapping of a far image point to a point close to the North Pole $\boldsymbol{N}$ of $\boldsymbol{S}$, for example, is less affected by noise and will thus inhere with a higher confidence, see figure 1. Mathematically, the uncertainties are computed using standard error propagation, where we profit from the inversion being an element of $\mathbb{G}_{4,1}$. Note that the obtained inhomogeneity in the uncertainties is one of main justifications for the use of the Gauss-Helmert method.

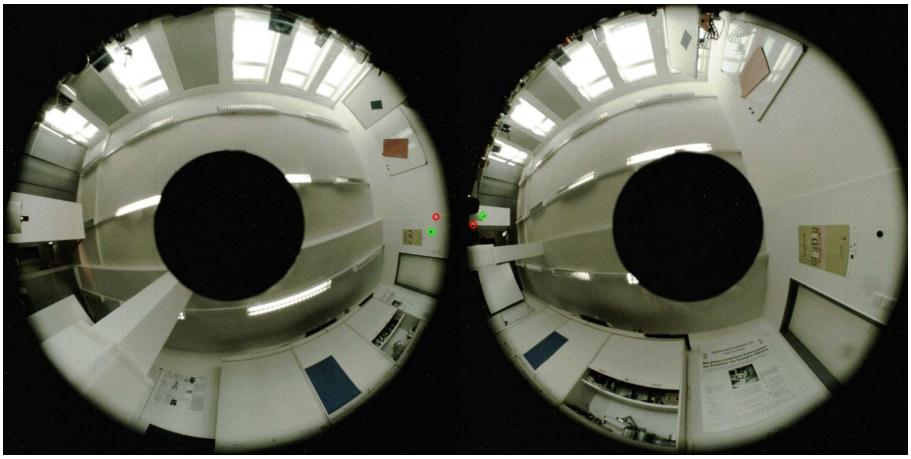

**Fig. 3.** The distance between the images is 3.5m. The distance and the ground truth epipoles were measured with a laser device. The red circles symbolize the epipoles found via the essential matrix. The green epipoles reflect the improved solutions of the Gauss-Helmert method. The difference seems to be small but an exact epipole is crucial for further processing.

The results of the Gauss-Helmert method can be seen in figure 3, which shows our most challenging scenario with a translation of 3.5m in between the camera positions. The red circles indicate the epipoles found via the essential

[5] This can be done as the true distance between $\boldsymbol{F}$ and $\boldsymbol{F}'$ cannot be recovered from the image data.

matrix approach described in section 5. The green circles show the stochastically optimal solution provided by the Gauss-Helmert method which exactly agree with the ground truth epipoles. These were determined with a laser along which the camera was moved. However, the uncertainty in the laser measured epipole positions is too big compared to the variation in the Gauss-Helmert results, which is why we do not state numerical results.

## 8 Conclusion

The objective of this work was to estimate the epipoles in omnidirectional images. The expression derived for the essential matrix is a new result and was shown to be correct. It gives some new insight into the structure of the essential matrix and enables a geometric interpretation. Concerning the fundamental matrix we identified an important connection to the work of Geyer and Daniilidis. We use the Gauss-Helmert method for the estimation of the stochastically optimal epipoles. As a byproduct we obtain the motion estimation between two omnidirectional images. The experimental results demonstrate that our method does provide exact results. Evidently, this work is also a valuable contribution to the field of (conformal) geometric algebra, which turned out to be the ideal framework to deal with geometry.

## References


1. Pierre Angles. Construction de revêtements du groupe conforme d'un espace vectoriel muni d'une ≪métrique≫ de type $(p, q)$. In *Annales de l'institut Henri Poincaré*, volume 33, pages 33–51, 1980.
2. Leo Dorst, Daniel Fontijne, and Stephen Mann. *Geometric Algebra for Computer Science: An Object-Oriented Approach to Geometry*. Morgan Kaufmann Publishers Inc., San Francisco, CA, USA, 2007.
3. Christopher Geyer and Konstantinos Daniilidis. Properties of the catadioptric fundamental matrix. In *7th European Conference on Computer Vision (ECCV), Copenhagen, Denmark*, pages 140–154, 2002.
4. Christopher Geyer and Kostas Daniilidis. Catadioptric projective geometry. *International Journal of Computer Vision*, 45(3):223–243, 2001.
5. D. Hestenes and G. Sobczyk. *Clifford Algebra to Geometric Calculus: A Unified Language for Mathematics and Physics*. Reidel, Dordrecht, 1984.
6. K.-R. Koch. *Parameter Estimation and Hypothesis Testing in Linear Models*. Springer, 1997.
7. Hongbo Li, David Hestenes, and Alyn Rockwood. Generalized homogeneous coordinates for computational geometry. In *Geometric computing with Clifford algebras: theoretical foundations and applications in computer vision and robotics*, pages 27–59. Springer-Verlag, London, UK, 2001.
8. Shree K. Nayar and Venkata Peri. Folded catadioptric cameras. In *Conference on Computer Vision and Pattern Recognition (CVPR), Ft. Collins, CO, USA*, pages 2217–, 1999.
9. T. Needham. *Visual Complex Analysis*. Clarendon Press, Oxford, 1997.
10. Faugeras Olivier. *Three-Dimensional Computer Vision*. MIT Press, 1993.

11. C. Perwass, C. Gebken, and G. Sommer. Estimation of geometric entities and operators from uncertain data. In *27. Symposium für Mustererkennung, DAGM 2005, Wien, 29.8.-2.9.005*, volume 3663 of *LNCS*, pages 459–467. Springer-Verlag, Berlin, Heidelberg, 2005.
12. B. Rosenhahn and G. Sommer. Pose estimation in conformal geometric algebra, part I: the stratification of mathematical spaces. In *Journal of Mathematical Imaging and Vision*, volume 22, pages 27–48. Springer Science + Business Media, Inc., 2005.
13. B. Rosenhahn and G. Sommer. Pose estimation in conformal geometric algebra, part II: real-time pose estimation using extended feature concepts. In *Journal of Mathematical Imaging and Vision*, volume 22, pages 49–70. Springer Science + Business Media, Inc., 2005.